BBA Advances 4 (2023) 100105

Contents lists available at ScienceDirect

BBA Advances

journal homepage: www.sciencedirect.com/journal/bba-advances

Loss of INPP5K attenuates IP_3-induced Ca^{2+} responses in the glioblastoma cell line U-251 MG cells

Jens Loncke [a], Tomas Luyten [a], Ana Raquel Ramos [b], Christophe Erneux [b], Geert Bultynck [a,*]

[a] Laboratory of Molecular and Cellular Signaling, KU Leuven, Leuven, Belgium
[b] ULB, IRIBHM, Campus Erasme, Bâtiment C, 808 Route de Lennik, Bruxelles 1070, Belgium

ARTICLE INFO

Keywords:
Calcium signaling
IP_3 receptors
Inositol polyphosphate 5-phosphatase K
$PI(4,5)P_2$

ABSTRACT

INPP5K (inositol polyphosphate 5-phosphatase K) is an endoplasmic reticulum (ER)-resident enzyme that acts as a phosphoinositide (PI) 5-phosphatase, capable of dephosphorylating various PIs including PI 4,5-bisphosphate ($PI(4,5)P_2$), a key phosphoinositide found in the plasma membrane. Given its ER localization and substrate specificity, INPP5K may play a role in ER-plasma membrane contact sites. Furthermore, $PI(4,5)P_2$ serves as a substrate for phospholipase C, an enzyme activated downstream of extracellular agonists acting on Gq-coupled receptors or tyrosine-kinase receptors, leading to IP_3 production and subsequent release of Ca^{2+} from the ER, the primary intracellular Ca^{2+} storage organelle. In this study, we investigated the impact of INPP5K on ER Ca^{2+} dynamics using a previously established INPP5K-knockdown U-251 MG glioblastoma cell model. We here describe that loss of INPP5K impairs agonist-induced, IP_3 receptor (IP_3R)-mediated Ca^{2+} mobilization in intact cells, while the ER Ca^{2+} content and store-operated Ca^{2+} influx remain unaffected. To further elucidate the underlying mechanisms, we examined Ca^{2+} release in permeabilized cells stimulated with exogenous IP_3. Interestingly, the absence of INPP5K also disrupted IP_3-induced Ca^{2+} release events. These results suggest that INPP5K may directly influence IP_3R activity through mechanisms yet to be resolved. The findings from this study point towards role of INPP5K in modulating ER calcium dynamics, particularly in relation to IP_3-mediated signaling pathways. However, further work is needed to establish the general nature of our findings and to unravel the exact molecular mechanisms underlying the interplay between INNP5K function and Ca^{2+} signaling.

1. Introduction

Phosphoinositide (PI) 5-phosphatases are a group of enzymes that dephosphorylate the 5-phosphate position of PIs, i.e. PI(3,5) bisphosphate (P_2), $PI(4,5)P_2$ and $PI(3,4,5)P_3$. Members include Lowe oculocerebrorenal syndrome protein (OCRL), inositol polyphosphate 5-phosphatase B (INPP5B), SH2-containing inositol 5-phosphatase1/2 (SHIP1/2), synaptojanin1/2 (SYNJ1/2), inositol polyphosphate 5-phosphatase E (INPP5E), proline rich inositol polyphosphate 5-phosphatase (INPP5J) and inositol polyphosphate 5-phosphatase K (INPP5K) [1]. INPP5K can use two lipid substrates $PI(4,5)P_2$ and $PI(3,4,5)P_3$ to generate PI4P and $PI(3,4)P_2$, respectively [2]. The human INPP5K is a 448 amino acid protein with an N-terminal catalytic domain and a INPP5K carboxy homology C-terminal domain responsible for protein-protein interactions as well as subcellular distribution of the phosphatase [2]. Most recent studies have concluded $PI(4,5)P_2$ to be the preferred substrate of the phosphatase [3–7]. With $PI(4,5)P_2$ as a substrate, INPP5K may control multiple signaling properties linked to a key PI, not only a precursor of both phospholipase C and class I PI 3-kinase, but also directly regulating the activity of several membrane channels and transporters [8,9]. INPP5K is highly expressed in developing and adult brain, eye and muscle [10]. Mutations in *INPP5K* cause a congenital muscular dystrophy syndrome with short stature, cataracts, and intellectual disability [11,12]. Most genetic mutations of INPP5K are missense mutations that occur in the catalytic domain and compromise the enzymatic activity [11,12]. Recent studies in skeletal muscle specific *INPP5K* knockout mice have shown a severe and progressive muscle disease, accompanied by marked lysosome depletion and autophagy inhibition due to the absence of $PI(4,5)P_2$ dephosphorylation [4]. INPP5K has been reported to localize in ruffles, in the nucleus but also at the surface of the endoplasmic reticulum (ER), a characteristic that is unique amongst the ten mammalian PI 5-phosphatases [3,13–15]. The localization of INPP5K at the ER results from an interaction with the protein ARL6IP1, a four-transmembrane ER protein

* Corresponding author.
E-mail address: geert.bultynck@kuleuven.be (G. Bultynck).

https://doi.org/10.1016/j.bbadva.2023.100105
Received 3 June 2023; Received in revised form 19 September 2023; Accepted 26 September 2023
Available online 27 September 2023

[3]. In HeLa cells, Dong et al. reported an increased abundance of ER sheets upon the loss of INPP5K by a siRNA-mediated knockdown approach [3]. The authors suggested that INPP5K participates in the fine control of ER organization. In the glioblastoma cell line, U-251 MG cells, the number of ER fragments significantly increased in INPP5K-depleted as compared to control cells [14]. This way, INPP5K might functionally impact cell homeostasis, as ER structural features and its many functional domains are important for cell survival and function. Particularly in the neuronal context, ER morphological changes are linked to an increased susceptibility to neurodegeneration [16]. The possibility exists that ER-anchored INPP5K would act on plasma membrane PI(4,5)P_2, as suggested in U-251 MG cells under particular conditions i.e. when cells were adhered to fibronectin [5]. The concept of a possible *trans* activity for INPP5K is also observed by other ER-attached phosphatases such as Sac1, a PI4P specific phosphatase, that acts on plasma membrane localized PI4P [17]. ER-plasma membrane contact sites also form microdomains for Ca^{2+} signaling, while Ca^{2+} signals themselves can shape ER-plasma membrane contact sites [18]. At ER-plasma membrane contact sites, the molecular key players for store-operated Ca^{2+} entry (SOCE) assemble. SOCE occurs upon interaction of the ER-resident protein STIM1 with plasmalemmal Orai1 Ca^{2+} channels [19,20]. These Ca^{2+} signals also impact several ER-plasmalemmal tethers as well as enzymes that influence the local lipid composition and lipid transfer between ER and plasma membrane [18]. Both STIM1 and Orai1 are also interacting with PIs: PI(4,5)P_2 can bind the polybasic region of STIM1 and PI4P, that is controlled by ER-Sac1 phosphatase, which may affect Orai-channel activity [19]. Also, the efficiency of agonist-induced Ca^{2+} signaling depends on the distance between plasma membrane, where PI(4,5)P2, the substrate of PLC to produce inositol 1,4,5-trisphosphate (IP_3) and the ER, the major intracellular Ca^{2+} store where the IP_3 receptors (IP_3Rs), IP_3-gated intracellular Ca^{2+}-release channels, are located. Cells in which the distance between plasma membrane and ER is increased display reduced rate of IP_3R-mediated Ca^{2+} rises evoked by agonists, as has been observed in protein kinase R-like endoplasmic reticulum kinase-deficient cells [21,22].

Given the preferential presence of INPP5K throughout the tubular ER [3], we asked whether INPP5K could have a functional role in ER Ca^{2+} dynamics. Thus, we examined whether the loss of INPP5K in U-251 MG cells could impact IP_3R-mediated, ER-originated Ca^{2+} signals evoked by agonists or originating from SOCE, which occurs upon ER Ca^{2+} depletion. Carbachol-induced Ca^{2+} responses were consistently lower in INPP5K-depleted cells, as compared to control cells and this appears to occur independently of modifications in total intracellular Ca^{2+} content between the two types of cells. The data provide a novel possible link between INPP5K lipid phosphatase and Ca^{2+} response to IP_3-mobilizing agonist(s) in U-251 MG cells. Additionally, we showed that a deficiency in INPP5K does not alter the process of SOCE, at least in the context of U-251 MG cells.

2. Materials and methods

2.1. Cell culture

U-251 MG shRNA scramble (shCTRL) and U-251 MG shINPP5K cells were transduced and selected as described in [5] and cultured in Dulbecco's modified Eagle's medium (DMEM), supplemented with 5% fetal bovine serum and 100 IU/mL penicillin and 100 μg/mL streptomycin (100x Pen/strep, Gibco/Invitrogen, Merelbeke, Belgium). Cells were maintained at 37 °C and 5% CO_2.

2.2. Intracellular Ca^{2+} measurements in intact cells

U-251 MG shRNA scramble and shINPP5K cells were seeded on black, F-bottom 96 well plates (Greiner Bio-One, Vilvoorde, Belgium) coated with 5 μg/mL bovine plasma fibronectin (Sigma, Overijse, Belgium). Cells were loaded with 1 μM Fura-2-AM (Eurogentec, Seraing, Belgium) in modified Krebs solution (150 mM NaCl, 5.9 mM KCl, 1.2 mM $MgCl_2$, 11.6 mM HEPES, 11.5 mM glucose and 1.5 mM $CaCl_2$, pH balanced at 7.3) at room temperature for 30 min. Subsequent de-esterification was performed in the absence of extracellular Fura-2-AM at room temperature for 30 min. 30 s after initiating acquisitions, extracellular Ca^{2+} was chelated with 3 mM EGTA in modified Krebs solution without added $CaCl_2$. To maintain chelating conditions, Ca^{2+} mobilizing agents were added in a 3 mM EGTA solution. Fluorescence was measured using a Flexstation 3 microplate reader (Molecular Devices, Sunnyvale, CA, USA) through alternating excitation of Fura-2 at 340 and 380 nm, while collecting emission at 510 nm.

2.3. $^{45}Ca^{2+}$ measurements in permeabilized cells

U-251 MG shRNA scramble and shINPP5K cells were seeded on 12-well plates coated with 5 μg/mL bovine plasma fibronectin (Sigma, Overijse, Belgium) 7 day prior to the $^{45}Ca^{2+}$ flux experiment. Cells were permeabilized with saponin (20 μg/mL) and non-mitochondrial Ca^{2+}stores were loaded with 150 nM $^{45}Ca^{2+}$ (28 μCi/mL) (PerkinElmer, NEZ013005MC, Waltham, MA, USA) for 45 min at 30 °C, in the presence of 10 mM NaN_3. Cells were washed with efflux medium containing 120 mM KCl, 30 mM imidazole hydrochloride, 1 mM EGTA, 4 μM thapsigargin and balanced at pH 6.8. $^{45}Ca^{2+}$ efflux was followed for 18 min by replacing the efflux medium every 2 min. After 10 min, different concentrations of IP_3 were added. Residual $^{45}Ca^{2+}$ was released by 2% sodium dodecyl sulfate addition for 30 min. Ca^{2+} release is displayed as a fractional loss, obtained by measuring the amount of Ca^{2+} released in 2 min over the total Ca^{2+} store content. IP_3-releasable Ca^{2+} was determined by subtracting the fractional loss after IP_3 addition with the fractional loss before IP_3 addition.

2.4. Western blotting

Cells were seeded on fibronectin coated (5 μg/mL) 6 well plates and grown until confluent. Cells were washed with phosphate-buffered saline and lysed with lysis buffer (50 mM Tris, 100 mM NaCl, 2 mM EDTA, 1% 3-[(3-*cholamidopropyl*)*dimethylammonio*]−1-propanesulfonate, 50 mM NaF, 1 mM Na_3VO_4, Pierce protease inhibitor tablets (Roche, Basel, Switzerland) at pH 7.4 for 30 min. Lysates were centrifuged at 5000 x g for 5 min and analyzed by Western blotting as described in [23]. 10 μg of protein lysate was loaded for all samples. Volumetric immunoblot quantification was performed using the ImageJ software [24]. The used antibodies were: rabbit homemade pan anti-IP_3R Rbt 475 [25] (1:1000) and mouse anti-actin (1:10 000) (Sigma, A5441, St Louis, MO, USA).

2.5. Results processing & statistical analysis

All statistical analyses were performed using the R software [26]. Anova fitting and assessment of normality and variance assumptions and Tukey-corrected post-hoc tests were performed using base R and the Anova function of the car package [27]. Plots displayed in this report were made with the ggplot2 package for R [28]. Dose-response curves were fitted using the drm function of the drc package for R [29].

Flexstation 3 data was pre-processed using custom-made Python scripts [30], making use of the NumPy [31] and Pandas [32] packages.

3. Results

In all the experiments, stable INPP5K depleted and control U-251 MG cells were used. The cells were generated via lentiviral transduction containing shRNA scramble (shCTRL) or a shRNA directed against INPP5K (shINPP5K) as previously described in [5,14]. Previously, Ramos et al. showed that in shINPP5K U-251 MG cells adhering to fibronectin, cell migration was decreased [5]. Because of the unique ER-localization of INPP5K among PI 5-phosphatases, we asked whether INPP5K could influence ER-originating Ca^{2+} signals. Additionally, the

implication of PIs in ER-PM contact and Stim/Orai regulation raised the question whether or not INPP5K could be involved in SOCE.

3.1. Loss of INPP5K leads to reduced IP_3R-mediated ER Ca^{2+} release without altering Ca^{2+} store content

To investigate IP_3R function, a selection of agonists was screened in FURA-2 loaded U-251 MG cells. We found that U-251 MG cells did not respond to either ATP, histamine, bradykinin or trypsin, suggesting these cells do not express purinergic, histamine, bradykinin or protease activated-receptors, respectively. However, the cells did respond to carbachol, an agonist of the acetylcholine receptors, which are coupled to G-proteins and stimulate phospholipase C-mediated IP_3 generation, in turn activating IP_3Rs [33]. A carbachol dose-response experiment in FURA-2 loaded cells was performed in the absence of extracellular Ca^{2+} to determine IP_3R-mediated Ca^{2+} release from intracellular stores without Ca^{2+} influx. Averaged traces of all experiments are displayed in Fig. 1A. Responses to different concentrations of carbachol were consistently lowered in shINPP5K cells (half maximal effective concentration (EC_{50}): 12.8 μM) compared to shCTRL cells (EC_{50}: 7.2 μM)

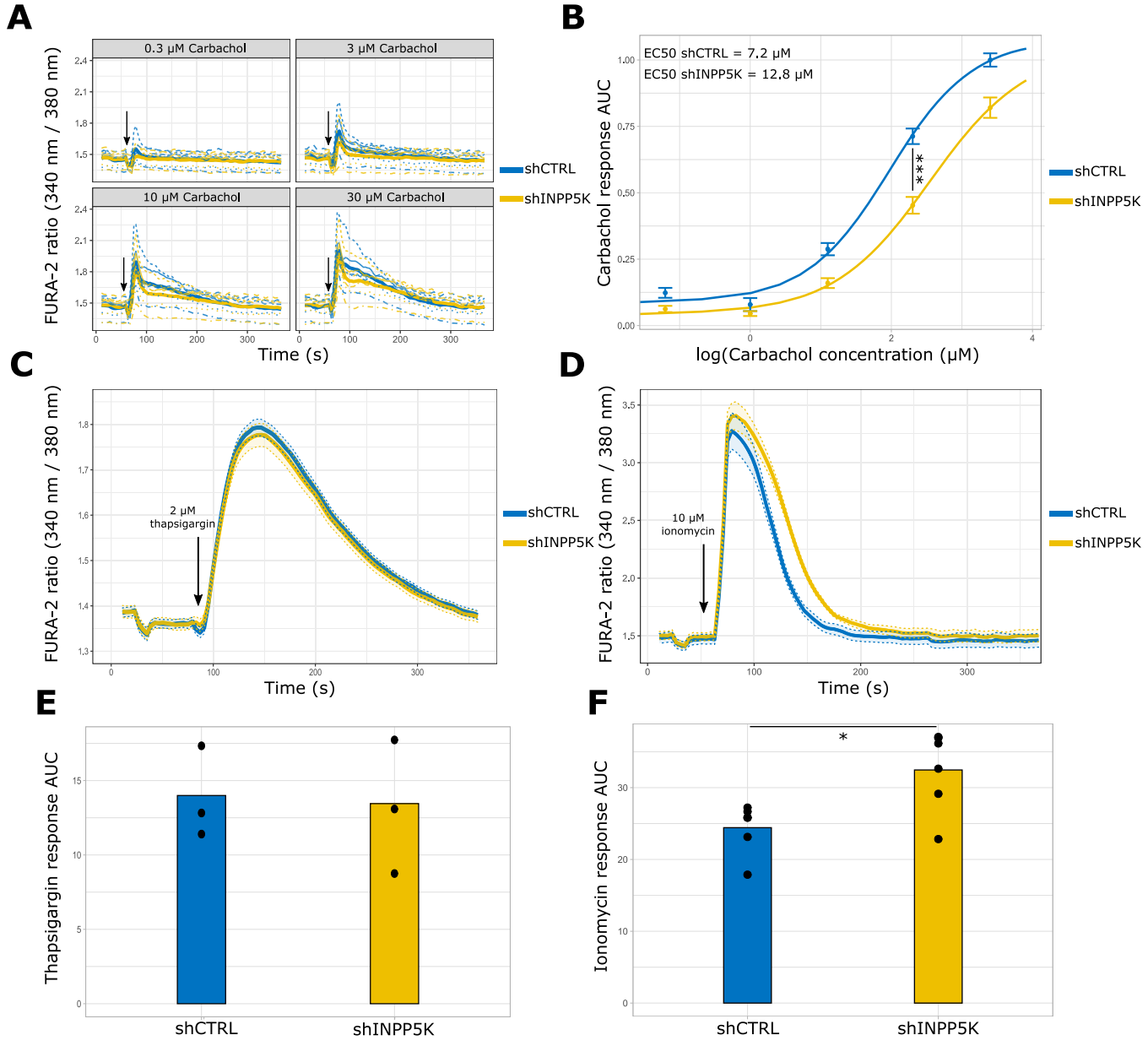

Fig. 1. IP_3R-mediated ER Ca^{2+} release is attenuated in shINPP5K cells. A: Averaged FURA-2 traces (thick lines) and individual N traces (thin lines) of shCTRL and shINPP5K U215 MG cell populations responding to different concentrations of carbachol, in the presence of 3 mM EGTA ($N = 6$). Black arrows indicate the time of carbachol addition. shCTRL and shINPP5K traces who were recorded simultaneously have the same line dash pattern. B: Dose response curve of area under curve (AUC) of carbachol reponses, normalized to response of shCTRL cells at 30 μM carbachol in the presence of 3 mM EGTA. The response to 10 μM carbachol is significantly decreased in shINPP5K cells ($p < 0.0001$), as assessed through a full factorial one-way ANOVA and subsequent Tukey-corrected pairwise post-hoc testing ($N = 6$). Error bars indicate mean +- standard error of mean. C: averaged FURA-2 traces (thick lines) with 95% confidence intervals (opaque ribbons) of cells treated with 2 μM thapsigargin in the presence of 3 mM EGTA ($N = 6$). D: averaged FURA-2 traces (thick lines) with 95% confidence intervals (opaque ribbons) of cells treated with 10 μM ionomycin in the presence of 3 mM EGTA ($N = 6$). E & F AUC of thapsigargin E and ionomycin (F) responses. Responses to ionomycin ($p = 0.017$) is significantly upregulated in shINPP5K cells, as assessed via an independent samples T-test ($N = 6$). Significant differences are annotated with asterisks (* $p < 0.05$, ** $p < 0.01$, *** $p < 0.001$).

(Fig. 1B). The representation of area under the curves in Fig. 1B was scaled to the average 30 μM carbachol response of shCTRL cells. The difference between EC_{50}'s was not significant (Mann-Whitney U test $w = 5$, p-value = 0.1508), however a full-factorial two-way Anova and Tukey-corrected post-hoc pairwise comparisons indicated a significantly lower response for shINPP5K cells when responding to 10 μM carbachol (adjusted p-value = 0.0002966). To determine ER Ca^{2+} store content we inhibited the sarco/endoplasmic reticulum Ca^{2+}ATPase (SERCA) through the addition of 2 μM thapsigargin in Ca^{2+} free conditions, visualized in Fig. 1C. Thapsigargin-releasable Ca^{2+} did not differ between shCTRL and shINPP5K cells (Fig. 1E), suggesting that decreased IP_3R-mediated Ca^{2+} release in INPP5K-deficient cells is not due to a lower ER Ca^{2+} store content. Similarly, total Ca^{2+} content was determined through addition of ionomycin in Ca^{2+} free conditions (Fig. 1D). shINPP5K cells had a significantly higher total Ca^{2+} content compared to shCTRL cells (independent samples T-test: t = -2.9692, p-value = 0.01703).

3.2. Reduced IP_3R-mediated ER Ca^{2+} release in INPP5K-deficient cells appears to be independent of IP_3R expression and IP_3 generation

We examined IP_3R protein expression levels through Western blotting and immunodetection using a pan-antibody against IP_3R recognizing all three isoforms (Fig. 2A). Volumetric quantification of IP_3R signal loading-corrected by B-actin staining (Fig. 2B) indicated that IP_3R expression levels were similar between shINPP5K and shCTRL cells. Thus, the aforementioned decreased IP_3R-mediated Ca^{2+} release is not manifested through decreased IP_3R expression. Next, we studied whether INPP5K could directly regulate IP_3R-mediated Ca^{2+} release, irrespective of IP_3 generation in permeabilized U-251 MG cells. We induced unidirectional $^{45}Ca^{2+}$ with either 1 μM IP_3, 10 μM IP_3 or the ionophore A23187 as a stimulus at the indicated time points (Fig. 2C). We quantified fractional loss normalized to Ca^{2+} released after ionophore stimulation (Fig. 2D), whereby a significantly lowered release with 1 μM IP_3 was visible for shINPP5K cells (Mann-Whitney U test: w = 3.6582, p-value = 0.007). Responses to ionophore were comparable between shINPP5K and shCTRL cells (Fig. 2E).

3.3. SOCE is unaffected by loss of INPP5K

We studied the process of SOCE by depleting FURA-2 loaded U-251 MG cells of Ca^{2+} by thapsigargin addition in Ca^{2+} free circumstances and a subsequent replenishment of intracellular Ca^{2+} by administration of excess extracellular Ca^{2+}, to overcome Ca^{2+}-chelating conditions (Fig. 3A). The supramaximal extracellular Ca^{2+} concentration of 50 mM used in the SOCE experiments is larger than physiological Ca^{2+} concentrations, though ensured maximal Ca^{2+} entry after store depletion and overcoming Ca^{2+}-chelating conditions. Both the magnitude of Ca^{2+}

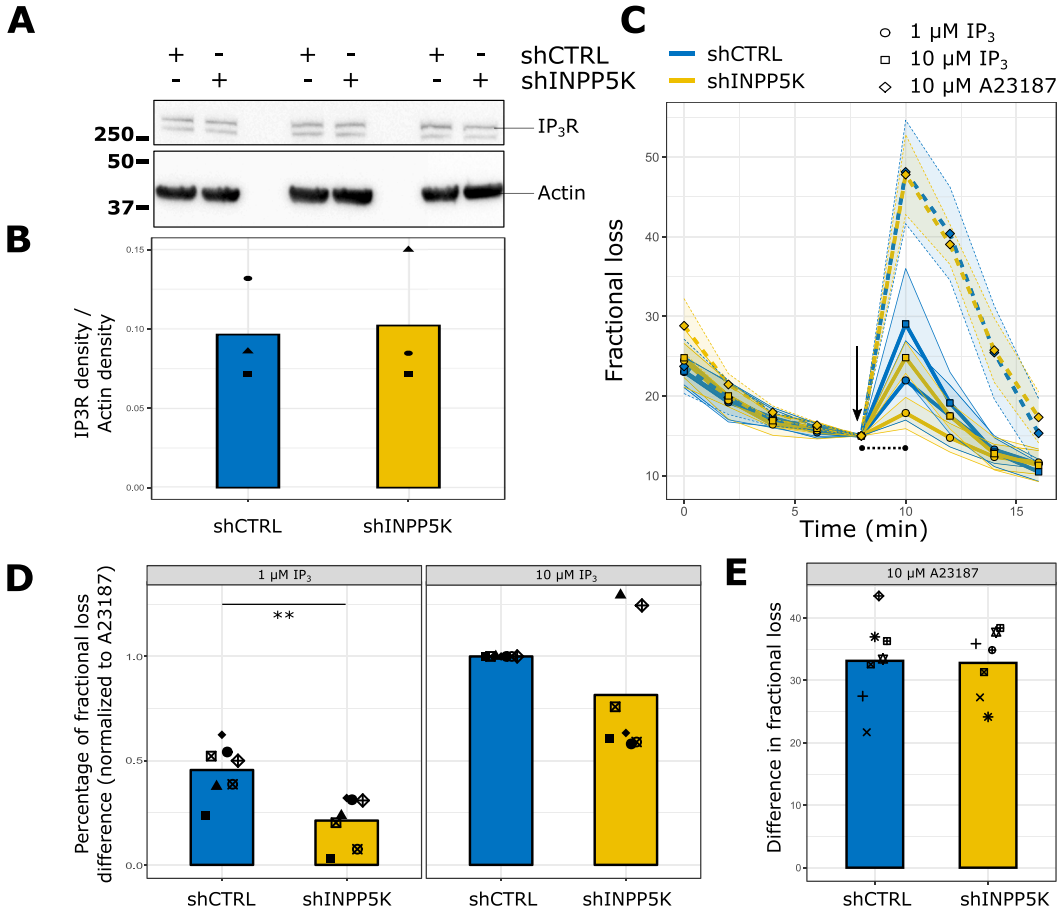

Fig. 2. Attenuated IP_3R-mediated ER Ca^{2+} release in shINPP5K cells is not attributable to decreased IP_3R protein expression, but likely in part attributable to decreased IP_3R sensitivity to IP_3. A: Immunoblot of lysates of shCTRL / shINPP5K U-251 MG stained with a pan-IP_3R and β-actin antibody. B: Volumetric quantification of immunoblot in A. IP_3R densities are displayed relative to actin densities ($N = 3$). C: Average fractional loss of $^{45}Ca^{2+}$as a function of time in permeabilized shCTRL / shINPP5K U-251 MG cells with 95% confidence intervals (opaque ribbons). Time of addition of IP_3 or A23187 is indicated by an arrow. Fractional loss at the time of addition of stimuli, indicated by a black arrow, is set at 15. Differences in fractional loss were quantified over two sampling points, as indicated by the black dashed line. D: Quantification of difference in fractional loss of $^{45}Ca^{2+}$ upon 1 and 10 μM IP_3 addition, normalized to A23187 ionophore and displayed relative to the shCTRL response to 10 μM IP_3 which was set to 1. Shapes of points correspond to different biological replicates ($N = 7$). E: Quantification of difference in fractional loss of $^{45}Ca^{2+}$ upon 10 μM A23187 addition. Shapes of points correspond to different biological replicates ($N = 7$).

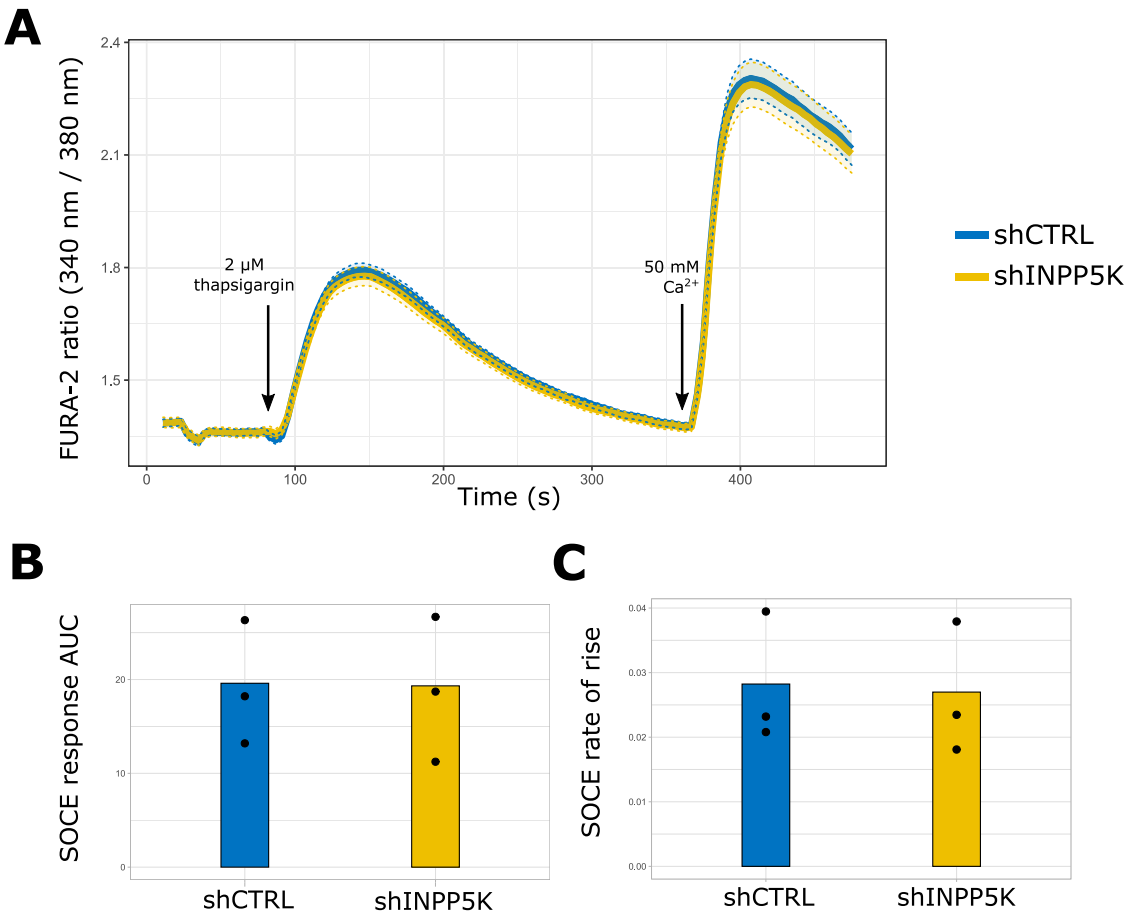

Fig. 3. Store-operated Ca^{2+} entry (SOCE) is unaffected by loss of INPP5K. A: Averaged FURA-2 traces (thick lines) with 95% confidence intervals (opaque ribbons) of cells treated with 2 μM thapsigargin followed by 50 mM Ca^{2+} in the presence of 3 mM EGTA ($N = 3$). B: Quantification of area under curve (AUC) and C: rate of rise after replenishment of Ca^{2+} after Ca^{2+} depletion.

reuptake (Fig. 3B) and the rate of rise (Fig. 3C) was similar between shINPP5K and shCTRL cells, suggesting that INPP5K is not involved in the process of SOCE at ER-PM contact sites.

4. Discussion

In this small, descriptive study, we provide evidence that INPP5K, which resides preferentially at the tubular ER, intersects with physiological Ca^{2+} signaling, thereby enhancing IP_3R-mediated Ca^{2+} release in the cellular context of a glioblastoma cell line, i.e. U-251 MG cells. Moreover, the decrease in IP_3R-mediated Ca^{2+} release upon loss of INPP5K is neither due to a reduction in intracellular Ca^{2+} store content, nor to a decrease in IP_3R-protein levels. When stimulating IP_3R directly with IP_3 in permeabilized cells, thus circumventing the need for the induction of signaling cascades leading to IP_3 generation, there was also a decreased IP_3R activity in INPP5K-deficient cells. Consequently, these results point towards a stimulatory role for INPP5K on IP_3R-mediated Ca^{2+} release, irrespective of Ca^{2+} store content. Finally, we found no evidence to support that INPP5K might be involved in SOCE.

Through dephosphorylation of PIs, PI 5-phosphatases exert their catalytic function on important second messengers in key cellular signaling pathways. PI 5-phosphatases are often enriched in membranes distal to the ER, in close proximity of their PI substrates [3]. A unique characteristic of INPP5K is that it is the sole member of the PI 5-phosphatase family that, at least partly, localized at the ER tubules [3]. Previously, it was shown that ER-anchored INPP5K could act *in trans* on plasma membrane $PI(4,5)P_2$, but solely under specific conditions, i.e. in U-251 MG cells adhered to fibronectin [5]. In the absence of fibronectin coating, no significant change in $PI(4,5)P_2$ between in U-251 shINPP5K and shCTRL cells was observed, in agreement with studies in HeLa cells [4,15]. At sites of ER-PM contact, a process termed SOCE occurs [34]. Upon depletion of ER Ca^{2+}, ER-localized STIM1 associates with PM Orai1 Ca^{2+} permeable channels to enable Ca^{2+} entry [34]. Of note, $PI(4,5)P_2$ binds the polybasic region of STIM1 [19]. Because of INPP5K localization and potential role in controlling $PI(4,5)P_2$ levels, we hypothesized that INPP5K could be involved in SOCE. By decreasing INPP5K expression in U-251 MG cells, adhered to fibronectin, we could not detect an effect on SOCE. This suggests the PI 5-phosphatase may not be a major regulator of SOCE.

We also measured IP_3R-mediated Ca^{2+} releases in U-251 MG cells adhered to fibronectin. By screening different agonists for IP3R stimulation, we found that U-251 MG cells responded to carbachol, but not to other known agonists of the IP_3R. This suggests that U-251 cells mainly activate IP_3Rs through acetylcholine receptor-mediated signaling. By evaluating carbachol responses in INPP5K-deficient cells, we found that particularly around the EC_{50}, INPP5K-deficient cells have a markedly decreased IP_3R-mediated Ca^{2+} release. Importantly, this was not due to a lower ER Ca^{2+} store content or an overall decreased Ca^{2+} store content. In fact, the response to ionomycin, an indicator for total Ca^{2+} store content, was even higher in shINPP5K cells compared to control cells. The decreased IP_3R mediated Ca^{2+} release was also not attributable to changed IP_3R protein levels or activity. This finding was somewhat surprising, since the absence of INPP5K is thought, in theory, to increase $PI(4,5)P_2$ levels, thus possibly increasing the pool of available substrate for phospholipase C to generate IP_3. In an attempt to elucidate whether somehow, an impaired IP_3 generation is introduced by depleting cells of

INPP5K, we directly stimulated IP_3Rs with IP_3 in permeabilized cells. A significantly decreased Ca^{2+} response to 1 μM IP_3 was observed, while also a non-significant trend was found using 10 μM IP_3. Therefore, INPP5K might have a direct effect on IP_3R-mediated Ca^{2+} fluxes, for instance by binding to the IP_3R, alone or as a part of a larger macrocomplex, as has been reported for various other regulators of the IP_3R, such as Neuronal Ca^{2+} Sensor 1 [35–37]. However, we cannot exclude that in intact cells loss of INPP5K also impairs the function of G-protein coupled receptors and downstream events such as IP_3 generation or IP_3 diffusion times, e.g. due to increased distances between ER and plasma membrane.

Dong et al. reported that depletion of INPP5K in HeLa cells resulted in an increase of ER sheets indicating a role of INPP5K in the fine control of ER organization (3). This was confirmed in our hands in U-251-MG cells adhered to fibronectin (5). Recent data reported in neurons of *C. elegans*, showed that the inositol PI 5-phosphatase, CIL-1 (ortholog of human INPP5K), functioned at the ER, regulated the cortical ER network, and maintained the distribution of ER-PM contacts in neurons [15]. In the absence of CIL-1, cortical ER sheets expanded with a concomitant reduction in ER tubules. The authors identified *cil-1* mutants with an early stop codon in the CIL-1 open reading frame or a mutation in the catalytic domain that exhibited abnormal distribution of the ER-PM contacts. No changes in the distribution PI(4,5)P2 had been detected in those *cil-1* mutants (using the pH domain derived from phospholipase C δ1 as probe), suggesting that the PI 5-phosphatase is capable of removing $PI(4,5)P_2$ in the ER without affecting $PI(4,5)P_2$ of the plasma membrane, thus acting primarily *in cis*. The minimal interpretation of the study is that CIL-1 is not acting through a detectable change in $PI(4,5)P_2$ [15]. Together the data suggest that the balance between ER sheets and tubules, which is INPP5K dependent, may determine where ER-PM contacts are distributed in neurons and perhaps other cells. Membrane contact sites are thus controlled by the PI 5-phosphatase expression that is targeted to the ER. Our data highlight a new role of INPP5K in the control of Ca^{2+} homeostasis i.e. deficiency in INPP5K leads to reduced IP_3R-mediated ER Ca^{2+} release. Given the function of INPP5K in human pathology i.e. muscular dystrophy and intellectual impairments [11,12], our observations, that need to be generalized to other cells, may therefore also play a role in proper axon regeneration. Indeed, alterations of structural features of the ER and ER Ca^{2+} homeostasis are intimately linked with neurodegeneration [16, 38], and our findings suggest INPP5K impacts both. Clearly, further work is needed to decipher the exact molecular mechanisms by which INPP5K controls IP_3R-mediated Ca^{2+} signaling and to understand the cell physiological consequences of the INPP5K/IP_3R interplay.

Finally, we wish to recognize that this short report is only descriptive, has several limitations and does not provide mechanistic insights in how INPP5K intersects with physiological Ca^{2+} signaling. However, we hope the results provide a stepping stone for others in the field for further investigations. Firstly, this report only focused on one cell model, namely U251-MG cells, in which INPP5K loss-of-function was previously studied [5]. Thus, it remains to be established on how generalizable these findings are towards other cellular and physiological systems. Secondly, the mechanisms by which INPP5K promotes IP_3R function remain unresolved and may be direct by forming a complex with IP_3Rs or indirect by impacting IP_3 signaling, lipid-dependent regulation of IP_3Rs, ER shape or properties of Ca^{2+} stores. Yet, the latter might be less likely given our findings in permeabilized cells using exogenously added IP_3. Hence, further work should examine whether IP_3Rs and INPP5K can form a molecular and functional complex. Thirdly, in this study, the cell physiological/biological consequences of INPP5K/IP_3R crosstalk and pathophysiological outcomes of deranged IP_3R function upon loss of INPP5K have not been addressed. In fact, PI 5-phosphatases including INPP5K control several cancer cell properties, such as cell migration, adhesion, polarity and cell invasion [39]. Moreover, loss of INPP5K deranged tip cell specification and impaired embryonic angiogenesis [40]. Loss-of-function mutations in INPP5K also cause congenital dystrophy [11]. However, the contribution of deranged IP_3R function in such cell systems and models remains to be established. Despite these limitations, the authors hope these results form a good basis for others to explore how INPP5K may impact cell function possibly through controlling IP_3R properties in future work. Given the retirement of Dr. Erneux, the authors wished to expose these results to the research community so others can build on and develop these findings.

Data availability

The underlying data will be available via KU Leuven RDR: https://doi.org/10.48804/8PANSC.

Author contributions

CE and GB conceived and participated in the design of the study. JL, TL and AR carried out experimental work. AR and CE provided critical reagents. JL drafted the manuscript and performed statistical analyses. JL, CE and GB interpreted results and determined the research strategy. CE and GB contributed to the drafting and amelioration of the manuscript. All authors read and approved the final manuscript.

Funding

Research in the authors' laboratories was supported by research grants from the Research Foundation – Flanders (FWO) (G.0818.21N, G.0945.22N to G.B., the Research Council – KU Leuven (C14/19/099 to G.B., the Eye Hope Foundation/Koning Boudewijnstichting (2020-J1160630-214966 to G.B.).

Declaration of Competing Interest

The authors declare that there is no conflict of interest.

Acknowledgments

We thank Anja Florizoone & Kirsten Welkenhuyzen for their excellent technical assistance.

References

[1] A.R. Ramos, S. Ghosh, C. Erneux, The impact of phosphoinositide 5-phosphatases on phosphoinositides in cell function and human disease, J. Lipid Res. 60 (2019) 276–286.
[2] S. Schurmans, C.A. Vande Catsyne, C. Desmet, B. Moës, The phosphoinositide 5-phosphatase INPP5K: from gene structure to in vivo functions, Adv. Biol. Regul. 79 (2021), 100760.
[3] R. Dong, T. Zhu, L. Benedetti, S. Gowrishankar, H. Deng, Y. Cai, X. Wang, K. Shen, P. De Camilli, The inositol 5-phosphatase INPP5K participates in the fine control of ER organization, J. Cell Biol. 217 (2018) 3577–3592.
[4] M.J. McGrath, M.J. Eramo, R. Gurung, A. Sriratana, S.M. Gehrig, G.S. Lynch, S. R. Lourdes, F. Koentgen, S.J. Feeney, M. Lazarou, C.A. McLean, C.A. Mitchell, Defective lysosome reformation during autophagy causes skeletal muscle disease, J. Clin. Investig. 131 (2021).
[5] A.R. Ramos, S. Ghosh, M. Dedobbeleer, P.A. Robe, B. Rogister, C. Erneux, Lipid phosphatases SKIP and SHIP2 regulate fibronectin-dependent cell migration in glioblastoma, FEBS J. 286 (2019) 1120–1135.
[6] A.C. Schmid, H.M. Wise, C.A. Mitchell, R. Nussbaum, R. Woscholski, Type II phosphoinositide 5-phosphatases have unique sensitivities towards fatty acid composition and head group phosphorylation, FEBS Lett. 576 (2004) 9–13.
[7] B. Moës, H. Li, P. Molina-Ortiz, C. Radermecker, A. Rosu, C.A. Vande Catsyne, S. A. Sayyed, J. Fontela, M. Duque, A. Mostafa, A. Azzi, J.T. Barata, R. Merino, C. Xu, C.J. Desmet, S. Schurmans, INPP5K controls the dynamic structure and signaling of wild-type and mutated, leukemia-associated IL-7 receptors, Blood 141 (2023) 1708–1717.
[8] J.G. Pemberton, Y.J. Kim, J. Humpolickova, A. Eisenreichova, N. Sengupta, D. J. Toth, E. Boura, T. Balla, Defining the subcellular distribution and metabolic channeling of phosphatidylinositol, J. Cell Biol. 219 (2020).
[9] M. Sohn, M. Korzeniowski, J.P. Zewe, R.C. Wills, G.R.V. Hammond, J. Humpolickova, L. Vrzal, D. Chalupska, V. Veverka, G.D. Fairn, E. Boura, T. Balla, $PI(4,5)P_2$ controls plasma membrane PI4P and PS levels via ORP5/8 recruitment to ER–PM contact sites, J. Cell Biol. 217 (2018) 1797–1813.

[10] T. Ijuin, Y. Mochizuki, K. Fukami, M. Funaki, T. Asano, T. Takenawa, Identification and characterization of a novel inositol polyphosphate 5-phosphatase, J. Biol. Chem. 275 (2000) 10870–10875.
[11] D.P.S. Osborn, H.L. Pond, N. Mazaheri, J. Dejardin, C.J. Munn, K. Mushref, E. S. Cauley, I. Moroni, M.B. Pasanisi, E.A. Sellars, R.S. Hill, J.N. Partlow, R. K. Willaert, J. Bharj, R.A. Malamiri, H. Galehdari, G. Shariati, R. Maroofian, M. Mora, L.E. Swan, T. Voit, F.J. Conti, Y. Jamshidi, M.C. Manzini, Mutations in *INPP5K* cause a form of congenital muscular dystrophy overlapping marinesco-sjögren syndrome and dystroglycanopathy, Am. J. Hum. Genet. 100 (2017) 537–545.
[12] M. Wiessner, A. Roos, C.J. Munn, R. Viswanathan, T. Whyte, D. Cox, B. Schoser, C. Sewry, H. Roper, R. Phadke, C. Marini Bettolo, R. Barresi, R. Charlton, C. G. Bönnemann, O. Abath Neto, U.C. Reed, E. Zanoteli, C. Araújo Martins Moreno, B. Ertl-Wagner, R. Stucka, C. De Goede, T. Borges da Silva, D. Hathazi, M. Dell'Aica, R.P. Zahedi, S. Thiele, J. Müller, H. Kingston, S. Müller, E. Curtis, M. C. Walter, T.M. Strom, V. Straub, K. Bushby, F. Muntoni, L.E. Swan, H. Lochmüller, J. Senderek, Mutations in *INPP5K*, encoding a phosphoinositide 5-phosphatase, cause congenital muscular dystrophy with cataracts and mild cognitive impairment, Am. J. Hum. Genet. 100 (2017) 523–536.
[13] R. Gurung, A. Tan, L.M. Ooms, M.J. McGrath, R.D. Huysmans, A.D. Munday, M. Prescott, J.C. Whisstock, C.A. Mitchell, Identification of a novel domain in two mammalian inositol-polyphosphate 5-phosphatases that mediates membrane ruffle localization. The inositol 5-phosphatase SKIP localizes to the endoplasmic reticulum and translocates to membrane ruffles following epidermal growth factor stimulation, J. Biol. Chem. 278 (2003) 11376–11385.
[14] A.R. Ramos, S. Ghosh, T. Suhel, C. Chevalier, E.O. Obeng, B. Fafilek, P. Krejci, B. Beck, C. Erneux, Phosphoinositide 5-phosphatases SKIP and SHIP2 in ruffles, the endoplasmic reticulum and the nucleus: an update, Adv. Biol. Regul. 75 (2020), 100660.
[15] J. Sun, R. Harion, T. Naito, Y. Saheki, INPP5K and Atlastin-1 maintain the nonuniform distribution of ER–plasma membrane contacts in neurons, Life Sci. Alliance 4 (2021), e202101092.
[16] S. Sree, I. Parkkinen, A. Their, M. Airavaara, E. Jokitalo, Morphological heterogeneity of the endoplasmic reticulum within neurons and its implications in neurodegeneration, Cells (2021).
[17] Y. Saheki, P. De Camilli, Endoplasmic reticulum–plasma membrane contact sites, Annu. Rev. Biochem. 86 (2017) 659–684.
[18] T. Balla, G. Gulyas, Y.J. Kim, J. Pemberton, Phosphoinositides and calcium signaling; a marriage arranged at ER-PM contact sites, Curr. Opin. Physiol. 17 (2020) 149–157.
[19] J.G. Pemberton, T. Balla, Polyphosphoinositide-binding domains: insights from peripheral membrane and lipid-transfer proteins, Adv. Exp. Med. Biol. 1111 (2019) 77–137.
[20] R.S. Lewis, Store-operated calcium channels: from function to structure and back again, Cold Spring Harb. Perspect. Biol. 12 (2020).
[21] G. Huang, J. Yao, W. Zeng, Y. Mizuno, K.E. Kamm, J.T. Stull, H.P. Harding, D. Ron, S. Muallem, ER stress disrupts Ca^{2+}-signaling complexes and Ca^{2+} regulation in secretory and muscle cells from PERK-knockout mice, J. Cell. Sci. 119 (2006) 153–161.
[22] A.R. Van Vliet, F. Giordano, S. Gerlo, I. Segura, S. Van Eygen, G. Molenberghs, S. Rocha, A. Houcine, R. Derua, T. Verfaillie, J. Vangindertael, H. De Keersmaecker, E. Waelkens, J. Tavernier, J. Hofkens, W. Annaert, P. Carmeliet, A. Samali, H. Mizuno, P. Agostinis, The ER stress sensor PERK coordinates ER-plasma membrane contact site formation through interaction with filamin-a and f-actin remodeling, Mol. Cell 65 (2017) 885–899, e886.
[23] G. Monaco, E. Decrock, H. Akl, R. Ponsaerts, T. Vervliet, T. Luyten, M. De Maeyer, L. Missiaen, C.W. Distelhorst, H. De Smedt, J.B. Parys, L. Leybaert, G. Bultynck, Selective regulation of IP_3-receptor-mediated Ca^{2+} signaling and apoptosis by the BH4 domain of Bcl-2 versus Bcl-Xl, Cell Death Differ. 19 (2012) 295–309.
[24] C.A. Schneider, W.S. Rasband, K.W. Eliceiri, NIH Image to ImageJ: 25 years of image analysis, Nat. Methods 9 (2012) 671–675.
[25] H.T. Ma, K. Venkatachalam, J.B. Parys, D.L. Gill, Modification of store-operated channel coupling and inositol trisphosphate receptor function by 2-aminoethoxy-diphenyl borate in DT40 lymphocytes, J. Biol. Chem. 277 (2002) 6915–6922.
[26] R.C. Team, R: A Language and Environment For Statistical Computing, R Foundation for Statistical Computing, Vienna, Austria, 2021.
[27] S.W. John Fox, An R Companion to Applied Regression, Sage, Thousand Oaks CA, 2019.
[28] H. Wickham, ggplot2: Elegant Graphics For Data Analysis, Springer-Verlag, 2016. Place Published.
[29] C. Ritz, F. Baty, J.C. Streibig, D. Gerhard, Dose-response analysis using R, PLoS One 10 (2016), e0146021.
[30] G. Van Rossum, F.L. Drake Jr, Python tutorial, Centrum voor Wiskunde en Informatica Amsterdam, Place Published, The Netherlands, 1995.
[31] C.R. Harris, K.J. Millman, S.J. van der Walt, R. Gommers, P. Virtanen, D. Cournapeau, E. Wieser, J. Taylor, S. Berg, N.J. Smith, R. Kern, M. Picus, S. Hoyer, M.H. van Kerkwijk, M. Brett, A. Haldane, J.F. del Río, M. Wiebe, P. Peterson, P. Gérard-Marchant, K. Sheppard, T. Reddy, W. Weckesser, H. Abbasi, C. Gohlke, T.E. Oliphant, Array programming with NumPy, Nature 585 (2020) 357–362.
[32] W. McKinney, Data structures for statistical computing in python place published, 2010.
[33] K. T S. Kobayashi, A.V. Somlyo, A.P. Somlyo, Cytosolic heparin inhibits muscarinic and alpha-adrenergic Ca^{2+} release in smooth muscle. Physiological role of inositol 1,4,5-trisphosphate in pharmacomechanical coupling, J. Biol. Chem. 264 (1989) 17997–18004.
[34] S.M. Emrich, R.E. Yoast, P. Xin, V. Arige, L.E. Wagner, N. Hempel, D.L. Gill, J. Sneyd, D.I. Yule, M. Trebak, Omnitemporal choreographies of all five STIM/Orai and IP_3Rs underlie the complexity of mammalian Ca^{2+} signaling, Cell Rep. 34 (2021).
[35] C. Angebault, J. Fauconnier, S. Patergnani, J. Rieusset, D. Danese, C. Affortit, J. Jagodzinska, C. Mégy, M. Quilès, C. Cazevieille, J. Korchagina, D. Bonnet-Wersinger, D. Milea, C. Hamel, P. Pinton, M. Thiry, A. Lacampagne, B. Delprat, C. Delettre, ER-mitochondria cross-talk is regulated by the Ca^{2+} sensor NCS1 and is impaired in Wolfram syndrome, Sci. Signal 11 (2018) eaaq1380.
[36] G.R. Boeckel, B.E. Ehrlich, NCS-1 is a regulator of calcium signaling in health and disease, Biochim. Biophys. Acta Mol. Cell Res. 1865 (2018) 1660–1667.
[37] L.D. Nguyen, E.T. Petri, L.K. Huynh, B.E. Ehrlich, Characterization of NCS1–$InsP_3R1$ interaction and its functional significance, J. Biol. Chem. 294 (2019) 18923–18933.
[38] P. Ilmari, T. Anna, A.M. Yasir, S. Sreesha, J. Eija, A. Mikko, Pharmacological regulation of endoplasmic reticulum structure and calcium dynamics: importance for neurodegenerative diseases, Pharmacol. Rev. 75 (2023) 959.
[39] A.R. Ramos, W.S. Elong Edimo, C. Erneux, Phosphoinositide 5-phosphatase activities control cell motility in glioblastoma: two phosphoinositides $PI(4,5)P_2$ and $PI(3,4)P_2$ are involved, Adv. Biol. Regul. 67 (2018) 40–48.
[40] E.M. Davies, R. Gurung, K.Q. Le, K.T.T. Roan, R.P. Harvey, G.M. Mitchell, Q. Schwarz, C.A. Mitchell, $PI(4,5)P_2$-dependent regulation of endothelial tip cell specification contributes to angiogenesis, Sci. Adv. 9 (2023) eadd6911.